Analytical Results about the Robustness of FMT Modulation with Several Prototype Pulses in Time-Frequency Selective Fading Channels

Andrea M. Tonello, *Member, IEEE,* and Francesco Pecile, *Student Member, IEEE*

***Abstract*— In this paper we study the performance of Filtered Multitone (FMT) modulation systems in time-frequency selective fading channels. FMT generalizes the OFDM scheme through the deployment of a sub-channel shaping pulse. A general analysis framework is reported, and it is specialized to the case of using a sinc pulse, a root-raised cosine pulse, and Gaussian pulse. Quasi-closed form expressions for the signal-to-interference (SIR) power ratio are derived. The results allow to benchmark the multitone system and understand how robust it is to frequency selective time-variant fading. We make a comparison with OFDM both in terms of SIR and bit-error-rate when single-tap sub-channel equalization is used. It shows that FMT can have better performance than OFDM due to the better sub-channel spectral containment. We also discuss the usefulness of the SIR results on the design of the prototype pulse in a time-frequency selective fading channel.**

***Index Terms*— DMT modulation, FMT modulation, fast fading, frequency selective fading, OFDM.**

I. Introduction

THE OBJECTIVE of this paper is the analysis of the performance of Filtered Multitone (FMT) modulation in time-variant frequency selective fading channels. FMT is a discrete-time implementation of multicarrier modulation that uses uniformly spaced sub-carriers and identical sub-channel pulses [1]-[2]. Orthogonal Frequency Division Multiplexing (OFDM) (also referred to as Discrete Multitone Modulation (DMT)) can be viewed as an FMT scheme that deploys rectangular time domain filters [3]. FMT has been originally proposed for application in broadband wireline channels [1], and subsequently it has been investigated for application in wireless channels [4]. A design approach is to use frequency confined pulses to get sub-channel orthogonality, and sub-channel equalization to cope with the inter-symbol interference (ISI) introduced by the channel.

The main research problems related to FMT are the efficient digital implementation, the design of the prototype pulse, the development of equalization schemes, and in general the performance analysis. A popular efficient polyphase filterbank architecture has been proposed by Cherubini *et al*. in [1]-[2]. The channel time-frequency selectivity may introduce inter-carrier interference (ICI) and ISI that can be minimized with the design of optimal time-frequency confined pulses. The pulse design problem in analog multicarrier systems has been treated by several authors [5]-[10]. Recently, simple pulse design criteria for FMT in frequency selective fading have been reported in [11]. Simplified sub-channel equalizers have been devised in [4], while optimal and iterative multi-channel equalizers have been proposed in [12]-[13]. Although multitone systems are robust to channel frequency selectivity, they are sensitive to carrier frequency offsets and phase noise, as well as to fast time variations of the channel impulse response [14]-[16]. An extensive literature exists on the performance analysis of multicarrier systems in time-variant frequency selective fading channels. However, this work does not consider the FMT scheme, rather it focuses on the specific OFDM solution where fast fading introduces ICI [17]-[24], while dispersive fading introduces both ICI and ISI when the cyclic prefix is shorter than the channel duration [16], [20].

In [25] we have studied the performance limits of FMT modulation, and we have shown that FMT provides both frequency and time diversity gains when optimal multi-channel equalization is used. However, if complexity is an issue, linear single channel equalizers are used. In this case the ICI can limit the performance.

Recently, Wang *et al*. have carried out a performance comparison between FMT and OFDM in time-variant frequency selective fading channels [26]. In [26] the results are obtained via numerical integration and are focused on an FMT system that uses a root-raised cosine pulse. In our paper, we provide a more general framework to the analysis of the SIR power ratio in FMT systems over time-variant frequency selective fading channels. The results are specialized when using sinc pulses (ideal FMT), Gaussian pulses, and root-raised cosine pulses. Closed (or quasi-closed) form expressions are found. The analysis methodology is extended to the OFDM solution, which allows to make a comparison between FMT and OFDM. It has both a theoretical and practical relevance since it allows to predict the bit-error-rate (BER) performance of FMT with known, and widely used, pulses when simple one tap equalization is implemented without resorting to time consuming Monte Carlo simulations. The analysis of the ISI and ICI power as a function of the system parameters gives guidelines on the design of the prototype pulse, and allows to understand whether more complex equalization, e.g., sub-

Manuscript submitted July 29, 2006; revised January 31, 2007 and July 30, 2007; accepted December 18, 2007. The editor coordinating the review of this paper and approving it for publication is V. Bhargava.

A.M. Tonello and F. Pecile are with DIEGM, Dipartimento di Ingegneria Elettrica Gestionale e Meccanica, University of Udine, Via delle Scienze 208, 33100, Udine, Italy (e-mail: {tonello, francesco.pecile}@uniud.it).

Digital Object Identifier 10.1109/TWC.2008.060528.

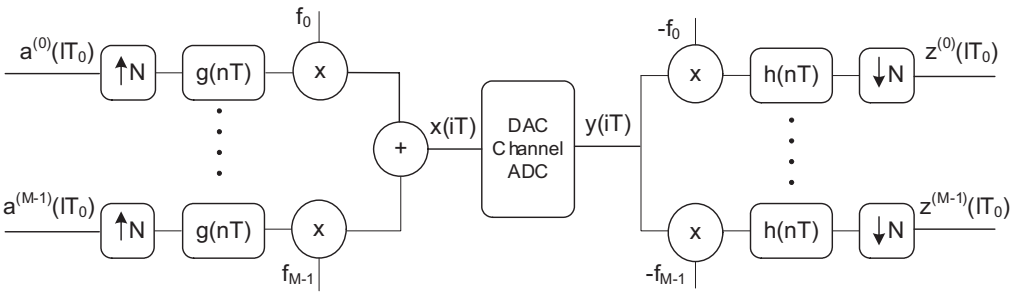

Fig. 1. FMT transmission system.

channel equalization, is required to yield low BER. To this respect, the best attainable performance is lower limited by the matched filter bound [25]. The analytical results of this paper yield, instead, an upper bound to the BER performance. Finally, as a by-product of the analysis, we obtain fast converging solutions to several definite integrals using expansions in series of functions.

This paper is organized as follows. In Section II, the system model is described. In Section III, we evaluate the output of the receiver filter bank when transmission is over a time-variant frequency selective channel. In Section IV, the average power of the signal and interference components is derived and specialized for several pulses. We discuss the results and we report a comparison with OFDM in Section V with reference to the SIR performance, and in Section VI with reference to the BER. Guidelines about the design of the prototype pulse are also discussed.

II. FMT Modulation Scheme

An FMT modulation based architecture [2],[25] is depicted in Fig. 1. The notation is summarized in Table I. The transmitter (synthesis stage) generates the signal

$$x(iT) = \sum_{k=0}^{M-1} \sum_{\ell \in \mathbb{Z}} a^{(k)}(\ell T_0) g(iT - \ell T_0) e^{j2\pi f_k iT} \quad i \in \mathbb{Z}, \quad (1)$$

where $a^{(k)}(\ell T_0)$ is the sequence of complex data symbols, e.g., M-QAM, that is transmitted on sub-channel $k = 0, ..., M-1$ at rate $1/T_0$. Furthermore, T is the sampling period[1], M is the number of sub-channels, $T_0 = NT$ is the sub-channel symbol period, with $K = N/M$ being the over sampling factor. The k-th sub-carrier has frequency $f_k = k/MT$, and $g(nT)$ is the prototype pulse. The transmission bandwidth is $W = 1/T$, and $R = M/T_0$ is the overall transmission rate in symbol/s.

The scheme is referred to as non-critically sampled FMT if the sub-carrier spacing $1/MT$ is larger than $1/T_0$. It is referred to as critically sampled FMT when $T_0 = MT$. A frequency guard equal to $f_G = 1/MT - (1+\alpha)/NT$ exists between sub-channels if the prototype pulse has confined frequency response with Nyquist band $1/T_0$, and roll-off α. The sub-carrier spacing decreases when we increase M, and we fix the transmission bandwidth. For a given band limited prototype pulse with Nyquist band $1/T_0$, the sub-channel bandwidth decreases by increasing N.

[1] T is assumed to be the time unit.

In this paper we specialize the performance analysis for the prototype pulses reported in Table I, that have both a practical and a theoretical relevance, i.e., the rectangular frequency domain pulse (Ideal FMT), the Gaussian pulse [25], the root-raised cosine (r.r.c.) pulse. We also use the rectangular pulse $g(nT) = \text{rect}\,(nT/T_0)$. In this case, (1) yields a cyclically prefixed (CP) OFDM signal with a CP of duration $\mu T = T_0 - MT$. While the prototype pulse is ideally band limited in FMT, in OFDM the sub-channels overlap because they have a sinc frequency response. Non-critically sampled FMT and CP-OFDM have the same transmission rate if they use the same number of tones and the same sub-channel symbol period T_0. In FMT some data rate penalty is due to the frequency guards (using an over sampling factor $N/M > 1$), in OFDM it is due to the CP.

A. Receiver Filter Bank

The signal (1) is digital-to-analog converted and transmitted over the communication channel (after RF conversion). The received lowpass signal is analog-to-digital converted to obtain $y(iT)$, and then it is passed through an analysis filter bank with prototype pulse $h(nT)$(Fig. 1). The sampled output, at rate $1/T_0$, corresponding to sub-channel k is

$$z^{(k)}(\ell T_0) = \sum_{i \in \mathbb{Z}} y(iT) e^{-j2\pi f_k iT} h(\ell T_0 - iT). \quad (2)$$

In FMT the analysis pulse is matched to the synthesis pulse, i.e., $h(nT) = g^*(-nT)$. In CP-OFDM the analysis pulse is $h(nT) = \text{rect}\,(-nT/MT)$ with $MT \le T_0 = (\mu + M)T$. The use of this analysis pulse corresponds to discard the cyclic prefix of duration $\mu T = (N - M)T$ at the beginning of the received block. Note that in CP-OFDM there is a sub-channel SNR penalty equal to M/N compared to FMT due to a receiver pulse that is not matched to the transmit pulse [25].

III. Receiver Filter Bank Output with Time-Frequency Selective Channel

We model the baseband channel with a discrete-time time-variant filter $g_{CH}(nT; mT)$ that comprises the effect of the DAC and ADC stages

$$g_{CH}(nT; mT) = \sum_{p \in P} \alpha_p(nT) \delta(m - p), \quad (3)$$

where $\delta(m)$ is the Kronecker delta. Assuming wide sense stationary scattering, the time-variant tap amplitudes $\alpha_p(nT)$,

TABLE I
NOTATION AND PROTOTYPE PULSE DEFINITIONS

NOTATION

T	sampling period
M	number of sub-channels
$T_0 = NT$	sub-channel symbol period with $K = N/M$ being the over sampling factor
f_k	k-th sub-carrier
$G(f)$	discrete-time Fourier transform of $g(nT)$
$\text{rep}_F(X(f))$	$= \sum_n X(f - nF)$, periodic repetition with period F
$\text{rect}(t)$	$= 1$ for $0 \le t < 1$, and zero otherwise
$\text{sinc}(t)$	$= \sin(\pi t)/(\pi t)$
$\text{rrcos}(t)$	$= \text{sinc}(\alpha t + 0.25)\sin(\pi(t - 0.25))/(4t)$ $+ \text{sinc}(\alpha t - 0.25)\sin(\pi(t + 0.25))/(4t)$
$RRCOS(f)$	$= \begin{cases} 1 & \text{for } 0 \le \lvert f\rvert < f_1, \\ 0 & \text{for } \lvert f\rvert > f_2, \\ \cos(\pi(\lvert f\rvert - f_1)/2\alpha) & \text{for } f_1 \le \lvert f\rvert < f_2, \end{cases}$ with $f_1 = 0.5 \times (1 - \alpha), f_2 = 0.5 \times (1 + \alpha)$
rcos(t)	$= 0.25 \times \pi\text{sinc}(t)(\text{sinc}(\alpha t + 0.5) + \text{sinc}(\alpha t - 0.5))$
Struve functions	$H_0(t) = \frac{4}{\pi}\sum_{k=0}^{\infty}\frac{J_{2k+1}(t)}{2k+1}$, $H_1(t) = \frac{2}{\pi} - \frac{2}{\pi}J_0(t) + \frac{4}{\pi}\sum_{k=1}^{\infty}\frac{J_{2k}(t)}{4k^2-1}$

PROTOTYPE PULSES

Rectangular frequency domain with bandwidth $1/T_0 \le 1/MT$	$g(nT) = \text{sinc}\left(\frac{nT}{T_0}\right)$ $G(f) = T_0\text{rep}_{1/T}\{\text{rect}(fT_0)\}$
Root-raised cosine with roll-off factor α, and bandwidth $(1 + \alpha)/T_0$	$g(nT) = \text{rrcos}\left(\frac{nT}{T_0}\right)$ $G(f) = T_0\text{rep}_{1/T}\{\text{RRCOS}(fT_0)\}$
Gaussian with equivalent band $B = f_{3dB}T_0$	$g(nT) = \sqrt{\frac{2\sigma}{\pi}}e^{-\left(\frac{\sigma nT}{T_0}\right)^2}$ $G(f) = \sqrt[4]{\frac{2\pi}{\sigma^2}}\text{rep}_{1/T}\left\{T_0 e^{-\left(\frac{f\pi T_0}{\sigma}\right)^2}\right\}$, with $\sigma = B\pi\sqrt{\frac{2}{\ln 2}}$
Rectangular in time domain	$g(nT) = \text{rect}(nT/T_0)$ $G(f) = T_0\text{sinc}(fT_0)$

$p \in P \subset \mathbb{Z}$, can be modeled as stationary complex Gaussian processes [18]. Further, with Clarke's isotropic scattering model [18], the tap amplitudes have zero mean, and correlation

$$\begin{aligned} r_{p,p'}(nT) &= E\left[\alpha_p(mT)^*\alpha_{p'}(mT + nT)\right] \\ &= \Omega_{p,p'}J_0(2\pi f_D nT), \end{aligned} \tag{4}$$

where $\Omega_{p,p'} = E\left[\alpha_p(mT)^*\alpha_{p'}(mT)\right]$, while f_D is the maximum Doppler, and $J_0(t)$ denotes the zero order Bessel function of the first kind [29]. Correlation among the T-spaced channel taps can be introduced by the filters in the ADC stage [17], [25]. The Delay-Doppler Spread Power Spectrum is obtained by the Fourier transform of (4), and it is equal to [18]

$$\begin{aligned} R_{p,p'}(f) &= \text{rep}_{\frac{1}{T}}\left\{\hat{R}_{p,p'}(f)\right\} \\ \text{with}\quad \hat{R}_{p,p'}(f) &= \begin{cases} \dfrac{\Omega_{p,p'}}{\pi f_D\sqrt{1 - (f/f_D)^2}} & \lvert f\rvert < f_D, \\ 0 & \text{otherwise.} \end{cases} \end{aligned} \tag{5}$$

It follows that the k-th sub-channel filter-bank output reads

$$\begin{aligned} z^{(k)}(\ell T_0) = &\sum_{\hat{k}=0}^{M-1}\sum_{m=-\infty}^{\infty} a^{(\hat{k})}(mT_0)g_{EQ}^{(\hat{k},k)}(\ell T_0; mT_0) \\ &+ \eta^{(k)}(\ell T_0), \end{aligned} \tag{6}$$

where $\eta^{(k)}(\ell T_0)$ is the Gaussian noise contribution, while the equivalent impulse response between the input sub-channel $\hat{k}$, and output sub-channel k is defined as

$$\begin{aligned} g_{EQ}^{(\hat{k},k)}(\ell T_0; mT_0) = &e^{j2\pi(f_{\hat{k}}mT_0 - f_k\ell T_0)}\sum_{i=-\infty}^{\infty} h^{(k)}(\ell T_0 - iT) \\ &\times \sum_p \alpha_p(iT)g^{(\hat{k})}(iT - pT - mT_0). \end{aligned} \tag{7}$$

In (7) we use the frequency shifted transmit and receive pulses that are defined respectively as

$$\begin{aligned} g^{(k)}(nT) &= g(nT)e^{j2\pi f_k nT}, \\ h^{(k)}(nT) &= h(nT)e^{j2\pi f_k nT}. \end{aligned} \tag{8}$$

Therefore, the output in the absence of noise can be written as

$$\begin{aligned} z^{(k)}(\ell T_0) = &a^{(k)}(\ell T_0)g_{EQ}^{(k,k)}(\ell T_0; \ell T_0) \\ &+ \underbrace{\sum_{m=-\infty, m\neq\ell}^{\infty} a^{(k)}(mT_0)g_{EQ}^{(k,k)}(\ell T_0; mT_0)}_{ISI^{(k)}(\ell T_0)} \\ &+ \underbrace{\sum_{\hat{k}\neq k}\sum_{m=-\infty}^{\infty} a^{(\hat{k})}(mT_0)g_{EQ}^{(\hat{k},k)}(\ell T_0; mT_0)}_{ICI^{(k)}(\ell T_0)}, \end{aligned} \tag{9}$$

where the first term represents the useful data contribution, the second additive term is the ISI contribution, the third term is the ICI contribution.

The objective of this paper is to determine the robustness of the system to the channel time and frequency selectivity as a function of the design parameters. To do so we evaluate the power of the interference components, which allows also to predict the BER performance as shown in Section VI. The analysis is quite general, and it is specialized to the pulses listed in Table I. In several cases, closed form expressions are found. In other cases, we pay particular attention to numerically compute definite integrals via series expansions that exhibit fast convergence and numerical stability.

IV. ANALYTICAL EVALUATION OF THE ISI AND ICI POWER

We note that the sub-channel sequence of samples at the receiver output can be written as

$$z^{(k)}(\ell T_0) = \sum_{\hat{k}=0}^{M-1} z^{(\hat{k},k)}(\ell T_0) + \eta^{(k)}(\ell T_0), \tag{10}$$

where

$$z^{(\hat{k},k)}(\ell T_0) = \sum_{m=-\infty}^{\infty} a^{(\hat{k})}(mT_0) g_{EQ}^{(\hat{k},k)}(\ell T_0; mT_0) \qquad (11)$$

is the contribution of the data stream transmitted on sub-channel $\hat{k}$ to the sub-channel analysis filter output of index k. We assume the data symbols to be i.i.d. with zero mean, and average power $M_a^{(k)} = E\left[|a^{(k)}(mT_0)|^2\right]$. Then, the average power of (11) equals

$$\begin{aligned} M_z^{(\hat{k},k)} &= E[|z^{(\hat{k},k)}(\ell T_0)|^2] \\ &= M_a^{(\hat{k})} \sum_m E\left[\left|g_{EQ}^{(\hat{k},k)}(\ell T_0; mT_0)\right|^2\right], \end{aligned} \qquad (12)$$

where the second equality holds with independent zero mean data symbols. The computation is independent of the time instant ℓT_0 because we are in stationary conditions, therefore we set $\ell = 0$. We refer to (12) as the *cross power* since it is the power of the interference on sub-channel k that is generated by sub-channel $\hat{k}$.

With the tapped delay line channel model, the cross power is

$$\begin{aligned} M_z^{(\hat{k},k)} = M_a^{(\hat{k})} &\sum_m \sum_{p,p'} \sum_{i,i'} r_{p,p'}(iT) \\ &\times g^{(\hat{k})}(iT + i'T - pT - mT_0) h^{(k)}(-iT - i'T) \\ &\times g^{(\hat{k})^*}(i'T - p'T - mT_0) h^{(k)^*}(-i'T). \end{aligned} \qquad (13)$$

It should be noted that if we fix $\hat{k} = k$ in (13), and we isolate the term that corresponds to $m = 0$, we obtain the average sub-channel signal power $S^{(k)} = M_a^{(k)} E\left[|g_{EQ}^{(k,k)}(0;0)|^2\right]$. The sum of all other terms yields the ISI power $M_{ISI}^{(k)} = E\left[|ISI^{(k)}(0)|^2\right]$, while the total power of the ICI can be obtained as $M_{ICI}^{(\hat{k})} = \sum_{\hat{k} \neq k} M_z^{(\hat{k},k)}$.

To proceed, we define the following *sub-channel product function*

$$gh^{(\hat{k},k)}(iT; sT) = g^{(\hat{k})}(iT - sT) h^{(k)}(-iT). \qquad (14)$$

Then, we can rewrite (13) as

$$\begin{aligned} M_z^{(\hat{k},k)} = \frac{M_a^{(\hat{k})}}{T} &\sum_m \sum_{p,p'} \sum_i r_{p,p'}(iT) \\ &\times c_{gh}^{(\hat{k},k)}(iT; pT + mT_0, p'T + mT_0), \end{aligned} \qquad (15)$$

where the deterministic autocorrelation of the sub-channel product function (14) is defined as

$$\begin{aligned} c_{gh}^{(\hat{k},k)}(iT; sT, s'T) = T \sum_{i'} &gh^{(\hat{k},k)}(iT + i'T; sT) \\ &\times gh^{(\hat{k},k)^*}(i'T; s'T). \end{aligned} \qquad (16)$$

The expression (15) is quite general, but it can be detailed for a certain choice of the sub-channel pulses. In certain cases, depending on the prototype pulse and the channel, it is convenient to calculate the cross power (15) partially in the frequency domain using the formula

$$\begin{aligned} M_z^{(\hat{k},k)} = \frac{M_a^{(\hat{k})}}{T} &\sum_m \sum_{p,p'} \sum_i r_{p,p'}(iT) \\ &\times \int_{-\frac{1}{2T}}^{\frac{1}{2T}} C_{gh}^{(\hat{k},k)}(f; pT + mT_0, p'T + mT_0) e^{j2\pi f iT} df, \end{aligned} \qquad (17)$$

or wholly in the frequency domain with the following formula that is obtained via the Parseval theorem

$$\begin{aligned} M_z^{(\hat{k},k)} = \frac{M_a^{(\hat{k})}}{T^2} &\sum_m \sum_{p,p'} \int_{-\frac{1}{2T}}^{\frac{1}{2T}} R_{p,p'}(-f) \\ &\times C_{gh}^{(\hat{k},k)}(f; pT + mT_0, p'T + mT_0) df. \end{aligned} \qquad (18)$$

In (17)-(18) we use the discrete-time Fourier transforms $C_{gh}^{(\hat{k},k)}(f; sT, s'T) = T \sum_n c_{gh}^{(\hat{k},k)}(nT; sT, s'T) e^{-j2\pi f nT}$, and $R_{p,p'}(f) = T \sum_n r_{p,p'}(nT) e^{-j2\pi f nT}$. The first transform can be written as

$$C_{gh}^{(\hat{k},k)}(f; sT, s'T) = GH^{(\hat{k},k)}(f; sT) GH^{(\hat{k},k)^*}(f; s'T), \qquad (19)$$

where $GH^{(\hat{k},k)}(f; sT)$ is the discrete-time Fourier transform of the product function (14), i.e.,

$$GH^{(\hat{k},k)}(f; sT) = \mathrm{rep}_{\frac{1}{T}}\left[\left(G^{(\hat{k})}(f) e^{-j2\pi f sT}\right) * H^{(k)}(-f)\right] \qquad (20)$$

and $G^{(k)}(f)$, $H^{(k)}(f)$ are the Fourier transforms of the frequency shifted pulses in (8). In the FMT scheme the receiver filter-bank is matched to the transmitter filter-bank, therefore, $H^{(k)}(f) = G^{(k)^*}(f)$.

In the following we specialize the results when the prototype pulse is sinc, Gaussian, and root-raised cosine (Table I). Further, we consider the channel to exhibit uncorrelated scattering so that the channel taps are statistically independent with zero mean, and power $\Omega_p = E[|\alpha_p(iT)|^2]$. This assumption is accurate as the signal bandwidth gets wide. It allows to simplify the analysis and acquire insights about the system performance. Data symbols with equal power, $M_a^{(k)} = M_a$, are also considered. With these assumptions the signal-to-interference power ratio (SIR) is identical on all sub-channels. When the channel taps are correlated the average SIR may vary across sub-channels as, for instance, shown in [25]. However, such a variation is small for typical wide band channels.

A. FMT with Sinc Pulse

With rectangular frequency domain pulses, the cross power equals (see the Appendix I)

$$\begin{aligned} M_z^{(\hat{k},k)} = \frac{M_a T_0^4}{T^2 \pi f_D} &\sum_m \sum_p \Omega_p \int_{-f_D}^{f_D} \frac{(|f + f_k - f_{\hat{k}}| - 1/T_0)^2}{\sqrt{1 - (f/f_D)^2}} \\ &\times \mathrm{sinc}^2\left((|f + f_k - f_{\hat{k}}| - \frac{1}{T_0})(pT + mT_0)\right) df. \end{aligned} \qquad (21)$$

It has been obtained starting from (18), and assuming stationary uncorrelated channel taps that exhibit a maximum Doppler smaller than the sub-carrier spacing, i.e., $f_D \leq 1/MT$.

Now, the sub-channel signal power can be computed by isolating the term in (21) of index $m = 0$, and setting $\hat{k} = k$. This yields

$$S^{(k)} = \frac{2M_a T_0^4}{T^2 \pi f_D} \sum_p \Omega_p \int_0^{f_D} \frac{(f - 1/T_0)^2}{\sqrt{1-(f/f_D)^2}} \times \text{sinc}^2\left((f - \frac{1}{T_0})pT\right) df. \quad (22)$$

The power of the sub-channel ISI is obtained from (21) as

$$M_{ISI}^{(k)} = \frac{2M_a T_0^4}{T^2 \pi f_D} \sum_{m\neq 0} \sum_p \Omega_p \int_0^{f_D} \frac{(f - 1/T_0)^2}{\sqrt{1-(f/f_D)^2}} \times \text{sinc}^2\left((f - \frac{1}{T_0})(pT + mT_0)\right) df. \quad (23)$$

Finally, the total power of the ICI experienced by a given sub-channel is

$$M_{ICI}^{(k)} = \sum_{\hat{k}\neq k} M_z^{(\hat{k},k)} = \frac{2M_a T_0^4}{T^2 \pi f_D} \sum_m \sum_p \Omega_p \int_{f_G}^{f_D} \frac{(f - f_G)^2}{\sqrt{1-(f/f_D)^2}} \times \text{sinc}^2\left((f - f_G)(pT + mT_0)\right) df. \quad (24)$$

It should be observed that (24) is always zero for $\hat{k} \neq k$ such that no ICI is present if $f_D \leq f_G = 1/MT - 1/T_0$, i.e., we use a frequency guard between sub-channels larger than the maximum Doppler. Otherwise, if $f_G < f_D \leq 1/MT$ only two adjacent sub-channels can generate ICI. Clearly, fast fading can introduce some ISI because it distorts the received sub-channel pulse as we will discuss in more detail in the following. Neither ISI nor ICI is present if the channel is flat and static.

B. FMT with Gaussian Pulse

Considering a Gaussian pulse, we obtain that the cross-channel power is (see the Appendix I)

$$M_z^{(\hat{k},k)} = \frac{M_a T_0^2}{T^2 \pi f_D} \sum_m \sum_p \Omega_p e^{-\left(\frac{sT\sigma}{T_0}\right)^2} \times \int_{-f_D}^{f_D} \frac{1}{\sqrt{1-(f/f_D)^2}} e^{-\left(\frac{\pi T_0 (f + f_k - f_{\hat{k}})}{\sigma}\right)^2} df, \quad (25)$$

where we assume that the pulse frequency response has extension smaller than $1/T$ such that its unfolded spectrum is limited in $[-1/2T, 1/2T)$.

Now, the signal power can be obtained from (25) by fixing $m = 0$, and setting $\hat{k} = k$

$$S^{(k)} = \frac{2M_a T_0^2}{T^2 \pi f_D} \sum_p \Omega_p e^{-\left(\frac{pT\sigma}{T_0}\right)^2} \times \int_0^{f_D} \frac{1}{\sqrt{1-(f/f_D)^2}} e^{-\left(\frac{\pi T_0 f}{\sigma}\right)^2} df. \quad (26)$$

The power of the sub-channel ISI is obtained from (25) and equals

$$M_{ISI}^{(k)} = \frac{2M_a T_0^2}{T^2 \pi f_D} \sum_{m\neq 0} \sum_p \Omega_p e^{-\left(\frac{(pT+mT_0)\sigma}{T_0}\right)^2} \times \int_0^{f_D} \frac{1}{\sqrt{1-(f/f_D)^2}} e^{-\left(\frac{\pi T_0 f}{\sigma}\right)^2} df. \quad (27)$$

The total power of the ICI is

$$M_{ICI}^{(k)} = \sum_{\hat{k}\neq k} M_z^{(\hat{k},k)} = \frac{M_a T_0^2}{T^2 \pi f_D} \sum_m \sum_p \Omega_p e^{-\left(\frac{(pT+mT_0)\sigma}{T_0}\right)^2} \times \sum_{\hat{k}\neq k} \int_{-f_D}^{f_D} \frac{1}{\sqrt{1-(f/f_D)^2}} e^{-\left(\frac{\pi T_0 (f + f_k - f_{\hat{k}})}{\sigma}\right)^2} df. \quad (28)$$

If we suppose that only two adjacent sub-channels can generate ICI, we can write (28) as follows

$$M_{ICI}^{(k)} = \frac{2M_a T_0^2}{T^2 \pi f_D} \sum_m \sum_p \Omega_p e^{-\left(\frac{(pT+mT_0)\sigma}{T_0}\right)^2} \times \int_{-f_D}^{f_D} \frac{1}{\sqrt{1-(f/f_D)^2}} e^{-\left(\frac{\pi T_0 (f+1/(MT))}{\sigma}\right)^2} df. \quad (29)$$

We observe that with Gaussian pulses we always experience some degree of ICI and ISI.

C. FMT with Root-Raised-Cosine Pulse

The computation of (18) requires some cumbersome algebra if we consider root-raised cosine pulses. We report some specific results in the Appendices I-III.

D. CP-OFDM Case

The general expression for the interference power in (15) can be used also to evaluate the power of the interference components in CP-OFDM. In CP-OFDM the sub-channel transmit pulse is rectangular with duration $T_0 = NT$, the cyclic prefix has duration $\mu = N - M$ samples, and the receiver pulse is rectangular with duration MT. Thus, from (15), the power of the interference seen by sub-channel k reads

$$M_z^{(\hat{k},k)} = M_a \sum_m \sum_p \sum_{i=0}^{M-1} \sum_{i'=0}^{M-1} r_{\alpha_p}(iT - i'T) \times e^{j2\pi(f_{\hat{k}} - f_k)(iT - i'T)} \times \text{rect}\left(\frac{iT + mT_0 + pT}{T_0}\right) \text{rect}\left(\frac{i'T + mT_0 + pT}{T_0}\right). \quad (30)$$

From (30) we can compute the power of the useful term, of the sub-channel ISI, and of the ICI, as follows:

$$S^{(k)} = M_a \sum_p \sum_{i=0}^{M-1} \sum_{i'=0}^{M-1} r_{\alpha_p}(iT - i'T) \times \text{rect}\left(\frac{iT + pT}{T_0}\right) \text{rect}\left(\frac{i'T + pT}{T_0}\right), \quad (31)$$

$$M_{ISI}^{(k)} = M_a \sum_{m\neq 0} \sum_{p} \sum_{i=0}^{M-1} \sum_{i'=0}^{M-1} r_{\alpha_p}(iT - i'T) \times \text{rect}\left(\frac{iT + mT_0 + pT}{T_0}\right) \text{rect}\left(\frac{i'T + mT_0 + pT}{T_0}\right), \quad (32)$$

$$M_{ICI}^{(k)} = M_{TOT}^{(k)} - S^{(k)} - M_{ISI}^{(k)}, \quad (33)$$

where the total power is

$$M_{TOT}^{(k)} = MM_a \sum_{m} \sum_{p} r_{\alpha_p}(0) \times \sum_{i'=0}^{M-1} \text{rect}^2\left(\frac{i'T + mT_0 + pT}{T_0}\right). \quad (34)$$

The above formulas generalize known results [18]-[24] on OFDM by taking into account both the presence of fast fading and multipath fading with time dispersion larger than the cyclic prefix.

V. SIR Evaluation

The results in the previous section allow the evaluation of the SIR power ratio on sub-channel k

$$SIR^{(k)} = \frac{S^{(k)}}{M_{ISI}^{(k)} + M_{ICI}^{(k)}}. \quad (35)$$

To compute (35) we need to numerically solve some integrals, e.g., the ones in (22)-(24), and in (26)-(29). This can be done by deriving equivalences that are obtained via series expansions [28]. To gain insight and distinguish between the effect of the delay spread and the Doppler spread, we consider first a multipath channel with quasi-static fading, and then a time-variant flat fading channel. Finally, we discuss the effects of a joint time and frequency selective fading channel. Quasi-closed form expressions (and in some cases, closed form expressions) for the SIR are derived in the Appendices II-III. The multipath channel is assumed to have power delay profile Ω_p with N_P independent taps having the Doppler spectrum in (5). Further, we assume identical signal power on all sub-channels. With these assumptions, the SIR is independent of the sub-channel index.

A. Frequency Selective Static Fading Channel

Let us assume the channel to be quasi-static but frequency selective. Then, it is possible to elaborate further (15), and obtain simple expressions for the signal and interference power in FMT. We report them in Appendix II. In Fig. 2.A, Fig. 2.B, and Fig. 3.A we show the SIR as a function of the normalized delay spread γ for the FMT system. We assume an exponential delay profile $\Omega_p \propto e^{-pT/(\gamma T)}$, and we truncate the channel at -20 dB. The series in (44) and (48)-(49) of the Appendix have fast convergence, so that they are computed for $|m| < 100$. In the figures, we fix the transmission bandwidth $1/T$, and the number of sub-channels $M = 32$, while we increase the factor N which implies that we compress the sub-channel bandwidth or equivalently we increase the sub-channel symbol period. It should be noted, that the delay spread is γT such that if the transmission bandwidth is 1 MHz, it equals 8 μs for $\gamma = 8$.

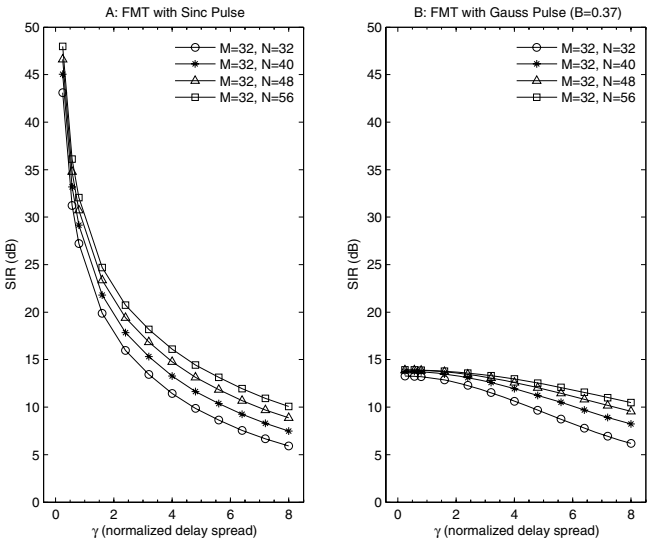

Fig. 2. SIR performance as a function of delay spread in frequency selective fading. FMT with sinc and Gaussian prototype pulse.

The figures show that the FMT architecture is robust to channel frequency selectivity. We can increase the sub-channel separation at the expense of data rate if we choose larger values of N. When the delay spread γ gets larger, the power of the ISI increases, thus the SIR decreases. It can be counteracted by using a higher number of sub-carriers (thus obtaining narrower sub-channels) or, if the SIR is particularly low, by using a sub-channel equalizer. The r.r.c. pulse (Fig. 3.A) and the sinc pulse (Fig. 2.A) have similar SIR performance. We point out that with these two pulses and the parameters used ($M = 32, N = 40, \alpha = 0.2$) the filter bank is with perfect reconstruction. The SIR degradation is entirely due to the channel selectivity. The SIR performance of the Gaussian pulse is rather poor. In this case a multi-channel equalizer is mandatory [12]-[13].

A comparison with CP-OFDM is shown in Fig. 3.B. In this case, the power of the useful term, the ISI and the ICI are computed from (31)-(33) and they are reported in Appendix II. In OFDM, when the channel is shorter than the CP, i.e., $N_p \leq \mu = N - M$, the ISI and ICI are zero. That is, the CP-OFDM system maintains the orthogonality [5]. But for channels longer than the CP it also suffers as a result of ISI and ICI. Now, comparing Fig. 3.A with Fig. 3.B, we can see that for small delay spreads CP-OFDM has better SIR performance than FMT, because the ISI is handled by the CP. However, as the delay spread increases and the channel becomes longer than the CP, OFDM also exhibits SIR floors. For instance, with $M = 32$ and $N = 40$, the SIR difference between OFDM and FMT is only 3 dB for $\gamma = 4$.

B. Flat Fast Fading Channel

Now, let us assume the channel to be flat but time-variant. Elaborating further the formulas of Section IV, we obtain simple SIR expressions that we report in Appendix III. We start this section discussing the results of Fig. 4 and Fig. 5 where we plot the SIR as a function of normalized Doppler $f_D T$. The curves start from $f_D T = 2 \times 10^{-6}$. With bandwidth

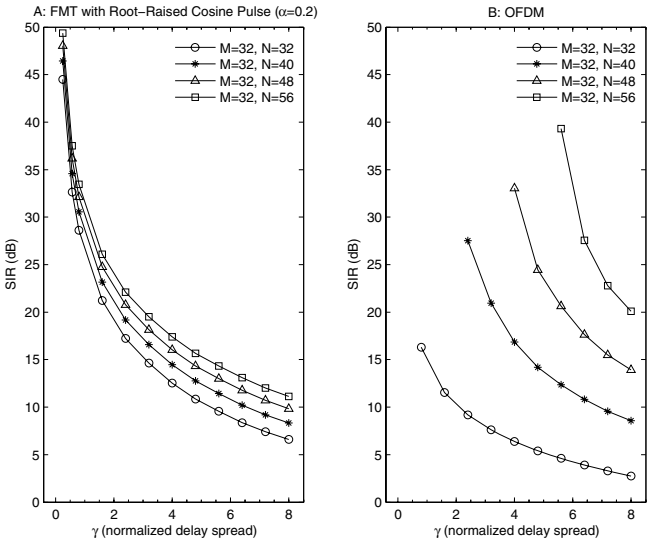

Fig. 3. SIR performance as a function of delay spread in frequency selective fading. FMT with root-raised-cosine pulse and OFDM with cyclic prefix of length *N-M* coefficients.

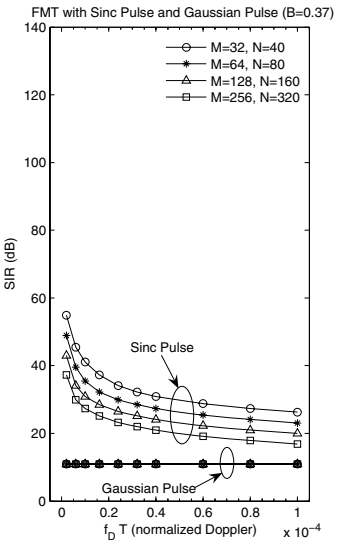

Fig. 4. SIR performance as a function of maximum Doppler in fast fading. FMT with sinc and Gaussian prototype pulse.

of 1 MHz, the Doppler equals 50 Hz when $f_D T = 5 \times 10^{-5}$.

Comparing Fig. 4 with Fig. 5.A, we see that the r.r.c. pulse yields much better SIR performance than the sinc and the Gaussian pulse. The gain ranges from a minimum of 20 dB up to 80 dB. It should be noted that the autocorrelation of the sinc pulse or the r.r.c. pulse is no longer an ISI free pulse in the presence of large Doppler, such that ISI is present and it lowers the SIR.

In Fig. 5.B we report SIR performance for the OFDM scheme. We see that OFDM is more robust than FMT with the sinc or the Gaussian pulse, but it performs significantly worse than FMT with the r.r.c. pulse. In this case, with $M = 32$ and $N = 40$, FMT exhibits 30 dB gain at $f_D T = 0.4 \times 10^{-4}$ over OFDM. In general, the SIR decreases as the number of tones increases in both systems. For moderate Doppler, since the ICI is negligible while the sub-channel impulse response is time-variant and dispersive, the performance of FMT can be improved with sub-channel adaptive equalization.

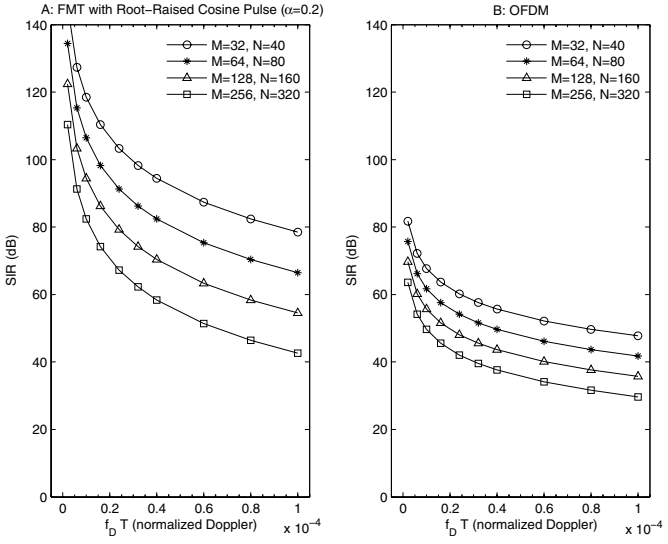

Fig. 5. SIR performance as a function of maximum Doppler in fast fading. FMT with root-raised-cosine pulse and OFDM.

C. Joint Time and Frequency Selective Fading Channel

The joint effect of the time and frequency channel selectivity is illustrated in Fig. 6. The SIR is plotted as a function of the normalized delay spread γ for several values of maximum Doppler $f_D T$. The plots show that the SIR for OFDM remains constant as the CP is longer than the channel. FMT has superior SIR performance for $\gamma < 1.5$ as a result of being more robust to channel time variations. Then, the two systems have similar performance. For the parameters herein considered, the FMT performance is dominated by the channel frequency selectivity if the normalized delay spread is larger than 1.5, while for $\gamma < 1.5$ it is the Doppler spread that lowers the SIR.

D. Considerations on the Prototype Pulse Design

The SIR results herein obtained can be used to guide the design of the prototype pulse and the choice of the system parameters. For a certain pulse, e.g., a root-raised cosine pulse, the formulas allow to determine the SIR as a function of the pulse duration, roll-off factor, number of tones, over sampling factor, and channel delay-Doppler spread. In particular, they allow to determine whether the ICI or the ISI dominates, and whether it is mostly caused by channel time variations or by frequency selectivity. As an example, we report the ISI/S and ICI/S ratios as a function of the length (Fig. 7.A, Fig. 7.B), and of the roll-off factor (Fig. 7.C, Fig. 7.D), of a truncated r.r.c. prototype pulse considering several values of delay-Doppler spread. Fig. 7.A shows that the ISI/S rapidly reaches a floor that equals the SIR^{-1} obtainable with an infinite length pulse (see Fig. 6.A). Fig. 7.B shows that if we increase the filter length we obtain a better frequency confinement so that the ICI/S decreases. For a given filter length, a different choice of the roll-off factor translates into a tradeoff between the amount of ISI and ICI that the system exhibits, as shown in Fig. 7.C

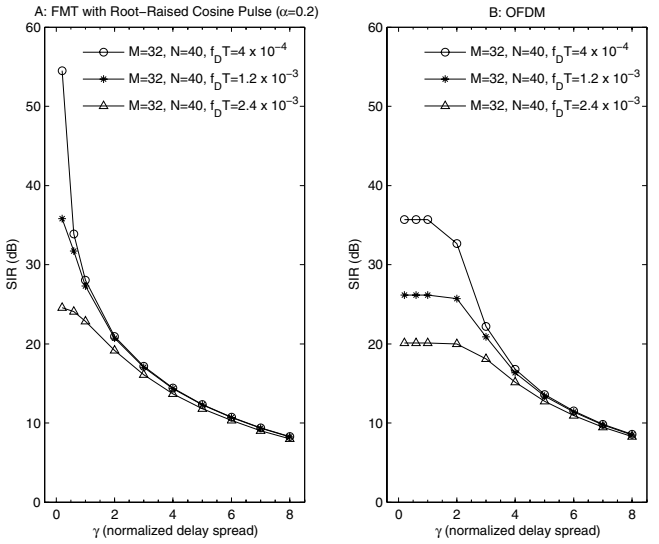

Fig. 6. SIR performance in a joint time-frequency selective fading channel. FMT with root-raised-cosine pulse and OFDM.

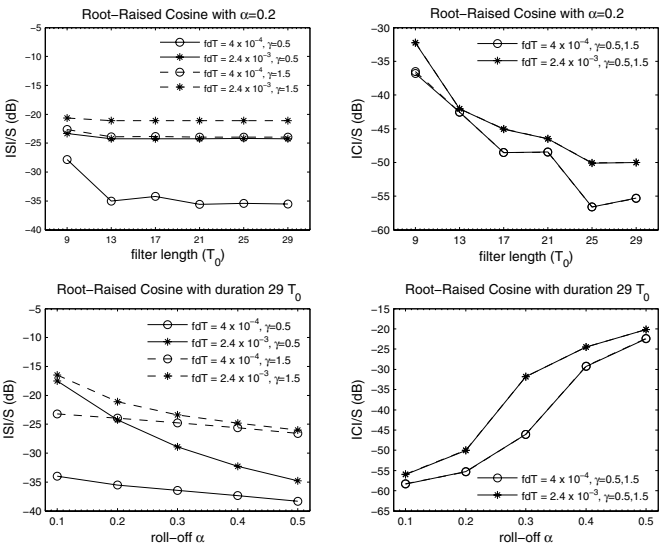

Fig. 7. ISI/S and ICI/S ratios as a function of the root-raised-cosine prototype filter length and roll-off factor in a joint time-frequency selective fading channel.

and 7.D. As we increase the roll-off, the excess bandwidth is increased, so that a higher overlapping of the sub-channel spectra is introduced, i.e., increased ICI. On the contrary, the impulse response has lower side lobes, so that we experience lower ISI.

The overall conclusion is that with a truncated r.r.c. pulse, the performance of FMT is bounded by the sub-channel ISI rather than by the ICI in time-frequency selective channels. It is interesting to note (see Figs. 2-5) that although the Gaussian pulse is a time-frequency confined pulse, it has poorer overall SIR performance than the band limited r.r.c. pulse in a time-frequency selective fading channel.

VI. BER Analysis

The SIR analysis of the previous section allows to predict the BER performance when single tap sub-channel equalization is used. That is, with the Gaussian approximation for the interference, and, for instance with 4-PSK modulation, the BER on sub-channel k can be approximated as follows [18]

$$BER^{(k)} = \frac{1}{2} - \frac{1}{2}\sqrt{\frac{1}{2}\left(\frac{1}{SIR^{(k)}} + \frac{1}{SNR^{(k)}}\right)^{-1}}. \quad (36)$$

We report in Fig. 8 and Fig. 9 a comparison between the theoretical BER (36), and the one that is obtained via a Monte Carlo simulation.

Now, in Fig. 8 we show the BER as a function of the signal-to-noise ratio for various values of normalized delay spread γ (with the same channel profile of Section V-A). With a transmission bandwidth equal to 1 MHz, the delay spread herein considered ranges between 2 μs to 5 μs. In Fig. 8.A we consider a 32 sub-channels FMT system with a r.r.c. pulse with roll-off 0.2, and with $N = 40$. In Fig. 8.B we consider OFDM with 32 tones and a CP of length 8. 4-PSK modulation is used. The two systems have identical data rate and deploy a single tap equalizer. The figure shows that in OFDM the theoretical and simulated curves are very close, while for FMT the discrepancy is more pronounced. This is due to the fact that in OFDM the Gaussian approximation is more accurate because a large number of intercarrier and intersymbol terms adds up to generate the interference. The error floor in the OFDM system for $\gamma = \{4, 5\}$ is due to the channel that has duration longer than the CP. The figure shows that FMT with single tap equalization performs well. As expected, the CP-OFDM system has better performance than FMT, i.e., it has lower error floors, for channels with duration close to the CP length. However, for channels in excess of the CP length, also the OFDM scheme exhibits high error floors and the performance of FMT and OFDM become similar.

In FMT more complex sub-channel equalization can yield lower BER. To this respect, the best attainable performance is lower bounded by the matched filter bound [25]. The analytical results of this paper yield, instead, an upper bound to the BER. To show this, we report the simulated performance of FMT using a 7 taps minimum-mean-square-error (MMSE) equalizer with ideal channel knowledge [18]. Now, with improved equalization FMT outperforms OFDM. Further, as the channel delay spread increases, better performance is exhibited because the equalizer provides frequency diversity gains [25], [27].

In Fig. 9 we make a comparison between FMT and OFDM in flat fast fading for various values of normalized Doppler $f_D T$. The comparison between Fig. 9.A and Fig. 9.B shows that in fast fading FMT with single tap equalization exhibits significantly lower error floors than OFDM.

In Fig. 10 we consider several combinations of Doppler and delay spread values. As the SIR analysis has already shown, single tap equalization in FMT is sufficient for $\gamma < 1.5$, and smaller losses than in OFDM are experienced as the Doppler spread increases. For $\gamma = 1.5$ the performance of FMT is dominated by the channel frequency selectivity while for OFDM by the time selectivity. For $\gamma > 1.5$, high error floors are exhibited by both systems although they are more pronounced in FMT with single tap equalization.

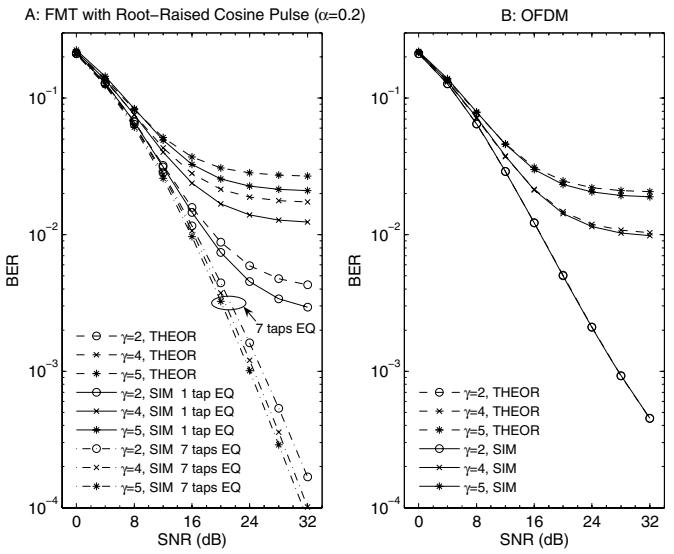

Fig. 8. BER for several values of delay spread. FMT with root-raised-cosine pulse and OFDM with cyclic prefix. The systems have M=32 and N=40. Both theoretical (THEOR) and simulated (SIM) curves are shown.

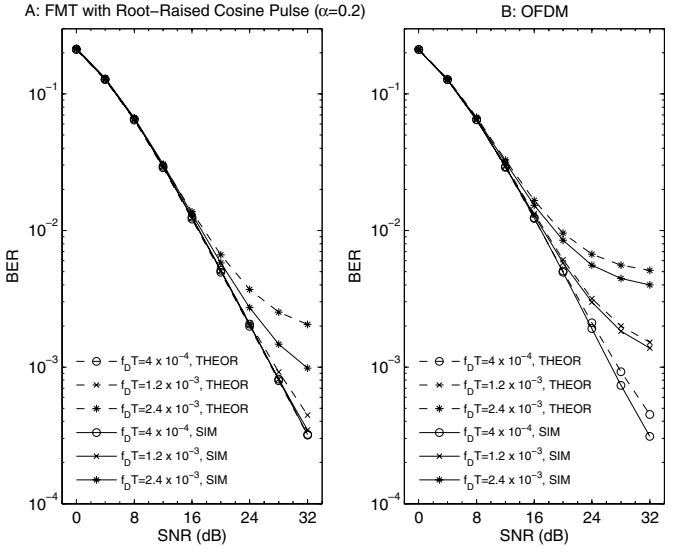

Fig. 9. BER for several values of maximum Doppler. FMT with root-raised-cosine pulse and OFDM with cyclic prefix. The systems have M=32 and N=40. Both theoretical (THEOR) and simulated (SIM) curves are shown.

VII. Conclusions

We have presented an analysis of the effect of time and frequency selectivity in FMT modulation schemes. We have obtained quasi-closed form expressions for the signal-to-interference power ratio. Particular attention has been paid to overcome the problems of accuracy in the numerical computation of the integrals. The results allow to characterize the effect of fading channels in these systems as a function of the parameters and the Doppler-delay spread. FMT deploys a frequency confined prototype pulse that makes the scheme robust to the inter-carrier interference generated by the channel time and frequency selectivity. Some ISI can arise but it can be handled with simple sub-channel equalization. In FMT, with a root-raised-cosine prototype pulse, a simple one tap equalizer is sufficient to yield superior SIR and BER performance than

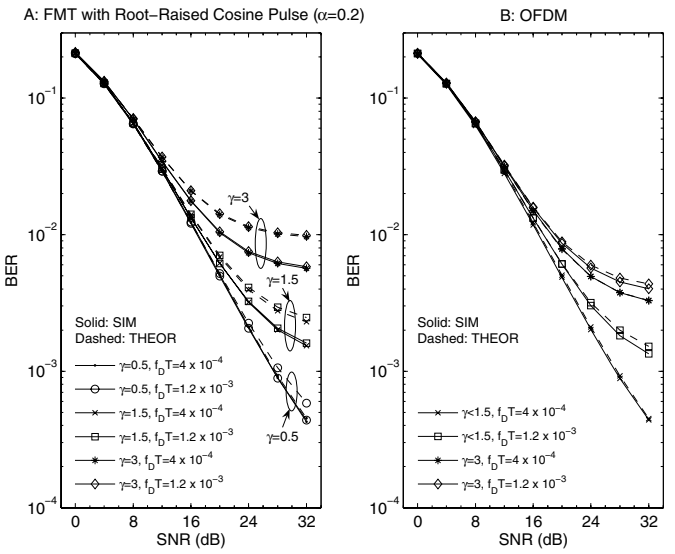

Fig. 10. BER for several values of maximum Doppler and delay spread. FMT with root-raised-cosine pulse and OFDM with cyclic prefix. The systems have M=32 and N=40. Both theoretical (THEOR) and simulated (SIM) curves are shown.

OFDM in fast fading. In frequency selective fading it achieves similar performance. The results also give guidelines on the design of the pulse, for instance, they allow to determine the length and roll-off factor of a r.r.c. pulse that yields a targeted amount of ICI and ISI in a time-frequency selective channel.

Appendix I
Interference Power for the FMT System

To calculate the interference power in the FMT case we need to evaluate $P(f;sT) = G^{(\hat{k})}(f)e^{-j2\pi fsT} * H^{(k)}(-f)$. This corresponds to (20) in a single period. The calculation needs some cumbersome algebra whose main steps are highlighted below for the pulses in Table I.

A. Sinc Pulse

$$P(f;sT) = T_0^2 \int_{-\infty}^{\infty} \text{rect}\,(T_0\lambda)\,\text{rect}\left(T_0\left(\lambda - f + f_{\hat{k}} - f_k\right)\right) \times e^{-j2\pi\lambda sT} d\lambda. \tag{37}$$

The integral (37) can be computed in closed form, which yields

$$P(f;sT) = \begin{cases} 0 & |f + f_k - f_{\hat{k}}| \geq 1/T_0 \\ P_-(f) = T_0^2/(2\pi sT) & \\ \times (e^{-j2\pi(f_{\hat{k}} - \frac{1}{2T_0})sT} & -1/T_0 \leq f + f_k - f_{\hat{k}} \leq 0 \\ -e^{-j2\pi(f+f_k+\frac{1}{2T_0})sT}) & \\ -e^{-j2\pi sT/T_0} P_-(f) & 0 \leq f + f_k - f_{\hat{k}} \leq 1/T_0 \end{cases} \tag{38}$$

The unfolded response $C_{gh}^{(\hat{k},k)}(f;sT)$ for $|f+f_k-f_{\hat{k}}| \leq 1/T_0$ equals:

$$C_{gh}^{(\hat{k},k)}(f;sT) = |P(f;sT)|^2 = T_0^4 \sin^2(\pi(|f+f_k-f_{\hat{k}}| - \frac{1}{T_0})sT)/(\pi sT)^2. \quad (39)$$

This expression can be substituted in (18) to obtain (21).

B. Gaussian Pulse

$$P(f;sT) = T_0 e^{-\frac{1}{2}\left(\frac{\left(\pi T_0^2(f+f_k-f_{\hat{k}})\right)^2 + j2\pi T_0^2 sT\sigma^2(f+f_k-f_{\hat{k}}) + \left(sT\sigma^2\right)^2}{\sigma^2 T_0^2}\right)}. \quad (40)$$

Consequently the calculation of $C_{gh}^{(\hat{k},k)}(f;sT)$ yields

$$C_{gh}^{(\hat{k},k)}(f;sT) = |P(f;sT)|^2 = T_0^2 e^{-\left(\frac{\left(\pi T_0^2(f+f_k-f_{\hat{k}})\right)^2 + \left(sT\sigma^2\right)^2}{\sigma^2 T_0^2}\right)}. \quad (41)$$

This expression can be substituted in (18) to obtain (25).

C. Root-Raised Cosine Pulse

$$P(f;sT) = T_0^2 \int_{-\infty}^{\infty} \text{RRCOS}(T_0\lambda) \times \text{RRCOS}\left(T_0\left(\lambda - f + f_{\hat{k}} - f_k\right)\right) e^{-j2\pi\lambda sT} d\lambda. \quad (42)$$

The result of this convolution is a piecewise trigonometric defined function. The same is for $C_{gh}^{(\hat{k},k)}(f;sT) = |P(f;sT)|^2$. Among the various intervals we are interested in $0 \leq \left|f+f_k-f_{\hat{k}}\right| \leq \alpha/T_0$ because the integral in (18) has extension limited by $|f| < f_D$. In general no closed form solution for (18) can be found. For particular cases, as for instance when we consider fast and flat fading (Section V-B), (18) can be expressed as a combination of Struve and Bessel functions [28]-[29].

Appendix II
Results in Frequency Selective Fading

In this Appendix we obtain analytical results about the signal and interference power in FMT assuming a frequency selective channel with uncorrelated quasi-static fading taps. The results have been used to plot Figs. 2-3.

A. Signal and Interference Power for FMT

When the channel is quasi-static but frequency selective with independent channel taps, the following simple expressions for the signal and interference power in FMT are obtained:

$$S_{FMT}^{(k)} = M_a \sum_{p=0}^{N_P} \Omega_p \left|k_g(-p)\right|^2, \quad (43)$$

$$M_{ISI-FMT}^{(k)} = M_a \sum_{m\neq 0} \sum_{p=0}^{N_P} \Omega_p \left|k_g(-mN-p)\right|^2, \quad (44)$$

where the prototype pulse autocorrelation is equal to

$$k_{sinc}(p) = N\text{sinc}\left(\frac{p}{N}\right), \quad (45)$$

$$k_{gauss}(p) = Ne^{-\frac{1}{2}\left(\frac{p}{N}\sigma\right)^2}, \quad (46)$$

$$k_{rrcos}(p) = N\text{rcos}\left(\frac{p}{N}\right), \quad (47)$$

when we assume a sinc, a Gaussian, and a r.r.c. prototype pulse. In (47) $\text{rcos}(t)$ denotes the impulse response of a raised cosine filter (see Table I).

With sinc and r.r.c. pulses the total power of the ICI is always zero assuming that the sub-carrier spacing is larger than $(1+\alpha)/T_0$. With a Gaussian pulse the ICI power is

$$M_{ICI-FMT}^{(k)} = M_a N^2 \sum_{m} \sum_{p=0}^{N_P} \Omega_p e^{-\left(\frac{(p+mN)\sigma}{N}\right)^2} \times \sum_{\hat{k}\neq k} e^{-\left(\frac{\pi T_0(f_k-f_{\hat{k}})}{\sigma}\right)^2}. \quad (48)$$

If we suppose that only two adjacent sub-channels can generate ICI we can write (48) as

$$M_{ICI-FMT}^{(k)} = 2M_a N^2 e^{-\left(\frac{\pi N}{\sigma M}\right)^2} \sum_{m} \sum_{p=0}^{N_P} \Omega_p e^{-\left(\frac{(p+mN)\sigma}{N}\right)^2}. \quad (49)$$

B. Signal and Interference Power for OFDM

For the frequency selective static fading channel herein considered, we can elaborate further (31)-(33) to obtain with OFDM

$$S_{OFDM}^{(k)} = M_a \sum_{p=0}^{\min(N-M,N_p)} \Omega_p M^2 + M_a \sum_{p=N-M+1}^{\min(N-1,N_p)} \Omega_p (N-p)^2, \quad (50)$$

$$M_{OFDM-ISI}^{(k)} = M_a \sum_{m\neq 0} \sum_{p=0}^{N_p} \Omega_p \times \sum_{i=0}^{M-1} \sum_{i'=0}^{M-1} \text{rect}\left(\frac{iT+mT_0+pT}{T_0}\right) \times \text{rect}\left(\frac{i'T+mT_0+pT}{T_0}\right), \quad (51)$$

$$M_{OFDM-ICI}^{(k)} = M_a \sum_{m} \sum_{p=0}^{N_p} \Omega_p \times \left(M - \sum_{i=0}^{M-1} \text{rect}\left(\frac{iT+mT_0+pT}{T_0}\right)\right) \times \sum_{i'=0}^{M-1} \text{rect}\left(\frac{i'T+mT_0+pT}{T_0}\right). \quad (52)$$

In (51)-(52) the sum in m has a finite number of terms depending on the channel duration. When the channel is shorter than the CP, i.e., $N_p \leq \mu = N - M$, the useful power is $S^{(k)} = M_a M^2 \sum_{p=0}^{N_P} \Omega_p$, while the ISI and ICI are zero. The formulas (50)-(52) give the power of the signal and the interference when the channel is longer than the CP [20].

APPENDIX III
RESULTS IN FAST FLAT FADING

In the following we report the analytical results that have been used to plot the curves in Fig. 4-5. They are derived under the assumption of fast flat fading with the Clarke's scattering model.

A. Sinc Pulse

With a sinc pulse the power of the useful term, of the ISI, and of the ICI read as follows

$$S_{FMT}^{(k)} = \frac{2M_a\Omega_0 N^4}{\pi}\left(\frac{(f_D T)^2\pi}{4} - \frac{2f_D T}{N} + \frac{\pi}{2N^2}\right), \quad (53)$$

$$M_{FMT-ISI}^{(k)} = \frac{M_a N^2 \Omega_0}{\pi^2}\sum_{m=1}^{\infty}\frac{1 - J_0(2\pi f_D m T_0)}{m^2}, \quad (54)$$

$$M_{FMT-ICI}^{(k)} = \frac{2M_a T_0^4 \Omega_0}{T^2 \pi f_D}\sum_m \int_{f_G}^{f_D} \frac{(f-f_G)^2}{\sqrt{1-(f/f_D)^2}} \times \operatorname{sinc}^2\left((f-f_G)mT_0\right) df. \quad (55)$$

Note that the power of the ICI (55) is zero when the sub-channels are separated by more than the maximum Doppler. Furthermore, note that the power of the useful signal is in closed form as a function of the maximum Doppler and of the parameter N. (53) and (54) have been obtained starting from (22)-(24) exploiting series of functions reported in [28].

B. Gaussian Pulse

With a Gaussian pulse, specializing (26)-(27) in fast flat fading, we obtain

$$S_{FMT}^{(k)} = M_a\Omega_0 N^2 e^{-\frac{1}{2}\left(\frac{\pi T_0 f_D}{\sigma}\right)^2} I_0\left(\frac{1}{2}\left(\frac{\pi T_0 f_D}{\sigma}\right)^2\right), \quad (56)$$

$$M_{FMT-ISI}^{(k)} = 2M_a\Omega_0 N^2 e^{-\frac{1}{2}\left(\frac{\pi T_0 f_D}{\sigma}\right)^2} \times I_0\left(\frac{1}{2}\left(\frac{\pi T_0 f_D}{\sigma}\right)^2\right)\sum_{m=1}^{\infty} e^{-(m\sigma)^2}, \quad (57)$$

where $I_0(t)$ is the zero-order modified Bessel function of the first kind [28]-[29]. The total power of the ICI from (29) equals

$$M_{FMT-ICI}^{(k)} = \frac{2M_a\Omega_0 N^2}{\pi f_D}\sum_m e^{-(m\sigma)^2}\int_{-f_D}^{f_D}\frac{1}{\sqrt{1-(f/f_D)^2}} \times e^{-\left(\frac{\pi T_0(f+1/(MT))}{\sigma}\right)^2} df. \quad (58)$$

Note that (56) and (57) differ from a constant factor that is equal to $2\sum_{m=1}^{\infty} e^{-(m\sigma)^2}$. Increasing σ reduces the ISI, but increases the ICI.

C. Root-Raised Cosine Pulse

With the r.r.c. pulse, the signal power in flat fast fading can be expressed as in (59) at the bottom of the page, where $H_{0,1}(t)$ are the Struve functions of order 0 and 1 which can be obtained from a series of Bessel functions of the first kind $J_k(t)$ and order k (see Table I, and [29], pp. 496-497).

The power of the ISI term has a complex expression that is still a combination of Bessel and Struve functions. It is omitted for space limits. The power of the ICI cannot be computed in closed form. However, $M_{FMT-ICI}^{(k)}$ is zero if the sub-channels are spaced more than the maximum Doppler.

D. Rect Pulse (CP-OFDM)

For the CP-OFDM system the power of the useful term and the ICI can be found from (31) and (33). The computation yields

$$S_{OFDM}^{(k)} = M_a\Omega_0 \sum_{i=0}^{M-1}\sum_{i'=0}^{M-1} J_0(2\pi f_D T(i-i')), \quad (60)$$

$$M_{OFDM-ICI}^{(k)} = M^2 M_a\Omega_0 - M_a\Omega_0\sum_{i=0}^{M-1}\sum_{i'=0}^{M-1} J_0(2\pi f_D T(i-i')). \quad (61)$$

The total power of the ISI is always zero. Note that (61) is identical to the one reported in [17].

REFERENCES

[1] G. Cherubini, E. Eleftheriou, S. Ölçer, and J. Cioffi, "Filter bank modulation techniques for very high speed digital subscriber lines," *IEEE Commun. Mag.*, vol. 38, no. 5, pp. 98-104, May 2000.

[2] G. Cherubini, E. Eleftheriou, and S. Ölçer, "Filtered multitone modulation for very high-speed digital subscriber lines," *IEEE J. Select. Areas Commun.*, vol. 20, no. 5, pp. 1016-1028, June 2002.

$$S_{FMT}^{(k)} = \frac{1}{4}\frac{M_a\Omega_0 N^2}{\pi^2}\Bigg[4\pi^2 + 6\alpha^2\pi^2 - 8\alpha\pi^2 + 32\alpha^2 + 3f_D^2 T_0^2\pi^2 - 32 f_D\pi T_0 + 32\alpha\pi(1-\alpha)H_0\left(f_D\pi\frac{T_0}{2\alpha}\right) + 16\alpha^2\pi H_0\left(f_D\pi\frac{T_0}{\alpha}\right) + 4f_D\alpha T_0\pi^2 H_1\left(f_D\pi\frac{T_0}{\alpha}\right) + 8f_D\pi^2 T_0 H_1\left(f_D\pi\frac{T_0}{2\alpha}\right) + (2f_D^2\pi^2 T_0^2 + 2\alpha^2\pi^2 - 32\alpha^2)J_0\left(f_D\pi\frac{T_0}{\alpha}\right) + (8f_D^2\pi^2 T_0^2 + 8\alpha\pi^2 - 8\alpha^2\pi^2)J_0\left(f_D\pi\frac{T_0}{2\alpha}\right) - 48T_0\alpha f_D\pi J_1\left(f_D\pi\frac{T_0}{2\alpha}\right) - 18T_0\alpha f_D\pi J_1\left(f_D\pi\frac{T_0}{\alpha}\right)\Bigg]. \quad (59)$$

[3] J. A. C. Bingham, "Multicarrier modulation for data transmission: an idea whose time has come," *IEEE Commun. Mag.*, vol. 28, no. 5, pp. 5-14, May 1990.

[4] N. Benvenuto, S. Tomasin, and L. Tomba, "Equalization methods in OFDM and FMT systems for broadband wireless communications," *IEEE Trans. Commun.*, vol. 50, no. 9, pp. 1413-1418, Sept. 2002.

[5] B. Le Floch, M. Alard, and C. Berrou, "Coded orthogonal frequency division multiplex [TV broadcasting]," *Proc. IEEE*, vol. 83, no. 6, pp. 982-996, June 1995.

[6] B. Le Floch, R. Halbert-Lassalle, and D. Castelain, "Digital sound broadcasting to mobile receivers," *IEEE Trans. Consumer Electron.*, vol. 35, no. 3, pp. 493-503, Aug. 1989.

[7] R. Haas and J.-C. Belfiore, "A time-frequency well-localized pulse for multiple carrier transmission," *Wireless Personal Commun.*, vol. 5, pp. 1-18, July 1997.

[8] W. Kozek and A. F. Molisch, "Nonorthogonal pulseshapes for multicarrier communications in doubly dispersive channels," *IEEE J. Select. Areas Commun.*, vol. 16, no. 8, pp. 1579-1589, Oct. 1998.

[9] D. Schafhuber, G. Matz, and F. Hlawatsch, "Pulse-shaping OFDM/BFDM systems for time-varying channels: ISI/ICI analysis, optimal pulse design, and efficient implementation," in *Proc. IEEE PIMRC '02*, vol. 3, pp. 1012-1016, Lisbon, Portugal, Sept. 2002.

[10] T. Strohmer and S. Beaver, "Optimal OFDM design for time-frequency dispersive channels," *IEEE Trans. Commun.*, vol. 51, no. 7, pp. 1111-1122, July 2003.

[11] B. Borna and T. N. Davidson, "Efficient design of FMT systems," *IEEE Trans. Commun.*, vol. 54, no. 5, pp. 794-797, May 2006.

[12] T. Hunziker and D. Dahlhaus, "Iterative detection for multicarrier transmission employing time-frequency concentrated pulses," *IEEE Trans. Commun.*, vol. 51, no. 4, pp. 641-651, April 2003.

[13] A. Tonello, "Asynchronous multicarrier multiple access: optimal and sub-optimal detection and decoding," *Bell Labs Techn. J.*, vol. 7, no. 3, pp. 191-217, 2003.

[14] L. Tomba and W. A. Krzymien, "Effect of carrier phase noise and frequency offset on the performance of multicarrier CDMA systems," in *Proc. IEEE ICC '96*, vol. 3, pp. 1513-1517, Dallas, TX, June 1996.

[15] A. Assalini, S. Pupolin, and A. M. Tonello, "Analysis of the effects of phase noise in filtered multitone (FMT) modulated systems," in *Proc. IEEE GLOBECOM '04*, vol. 6, pp. 3541-3545, Dallas, TX Nov. 2004.

[16] M. Speth, S. A. Fechtel, G. Fock, and H. Meyr, "Optimum receiver design for wireless broad-band systems using OFDM–part I," *IEEE Trans. Commun.*, vol. 47, no. 11, pp. 1668-1677, Nov. 1999.

[17] M. Russell and G. L. Stuber, "Interchannel interference analysis of OFDM in a mobile environment," in *Proc. IEEE Vehic. Tech. Conf. '95*, vol. 2, pp. 820-824, Chicago, IL, July 1995.

[18] G. L. Stuber, *Principles of Mobile Communications*. Kluwer, 1996.

[19] S. N. Diggavi, "Analysis of multicarrier transmission in time-varying channels," in *Proc. ICC '97*, vol. 3, pp. 1191-1195, Montreal, Canada, June 1997.

[20] H. Steendam and M. Moeneclaey, "Analysis and optimization of the performance of OFDM on frequency-selective time-selective fading channels," *IEEE Trans. Commun.*, vol. 47, no. 12, pp. 1811-1819, Dec. 1999.

[21] B. Stantchev and G. Fettweis, "Time-variant distortions in OFDM," *IEEE Commun. Lett.*, vol. 4, no. 10, pp. 312-314, Oct. 2000.

[22] Y. Li and L. J. Cimini, "Bounds on the interchannel interference of OFDM in time-varying impairments," *IEEE Trans. Commun.*, vol. 49, no. 3, pp. 401-404, Mar. 2001.

[23] Y.-S. Choi, P. J. Voltz, and F. A. Cassara, "On channel estimation and detection for multicarrier signals in fast and selective Rayleigh fading channels," *IEEE Trans. Commun.*, vol. 49, no. 8, pp. 1375-1387, Aug. 2001.

[24] X. Cai and G. B. Giannakis, "Bounding performance and suppressing intercarrier interference in wireless mobile OFDM," *IEEE Trans. Commun.*, vol. 51, no. 12, pp. 2047-2056, Dec. 2003.

[25] A. M. Tonello, "Performance limits for filtered multitone modulation in fading channels," *IEEE Trans. Wireless Commun.*, vol. 4, no. 5, pp. 2121-2135, Sept. 2005.

[26] T. Wang, J. G. Proakis, and J. R. Zeidler, "Interference analysis of filtered multitone modulation over time-varying fading channels," in *Proc. IEEE GLOBECOM '05*, vol. 6, pp. 3586-3591, St.Louis, MO, Nov. 2005.

[27] A. M. Tonello, "A concatenated multitone multiple-antenna air-interface for the asynchronous multiple-access channel," *IEEE J. Select. Areas Commun.*, vol. 24, no. 3, pp. 457-469, Mar. 2006.

[28] I. S. Gradshteyn and I. M. Ryzhik, *Table of Integrals, Series, and Products*. Academic Press, 4^{th}ed., 1983.

[29] M. Abramowitz and I. Stegun, *Handbook of Mathematical Functions*. New York: Dover Publ., 1970.

Andrea M. Tonello (M'00) received the Doctor of Engineering Degree in Electronics (cum laude) in 1996, and the Doctor of Research Degree in Electronics and Telecommunications in 2002 both from the University of Padova, Italy. On February 1997 he joined as a Member of Technical Staff, Bell Labs - Lucent Technologies where he worked on the development of base band algorithms for cellular handsets first in Holmdel, NJ, and then within the Philips/Lucent Consumer Products Division in Piscataway, NJ. From September 1997 to December 2002 he has been with the Bell Labs Advanced Wireless Technology Laboratory, Whippany, NJ. He was promoted in 2002 to Technical Manager, and was appointed Managing Director of Bell Labs Italy. On January 2003 he joined the Dipartimento di Ingegneria Elettrica, Gestionale e Meccanica (DIEGM) of the University of Udine, Italy, where he is currently an aggregate professor. Dr. Tonello is the author of several papers and patents. He has been involved in the standardization activity for the evolution of the IS-136 TDMA technology within UWCC/TIA. He received a Lucent Bell Labs recognition of excellence award for his work on enhanced receiver techniques. He is involved in several research projects related to wireless and powerline communications. He has been a TPC member of several conferences. He served as TPC Co-chair of the IEEE International Symposium on Power Line Communications 2007. He is a TPC Co-Chair of the IEEE Globecom 2008 General Symposium track on Emerging Technologies for Access and Home Networks. He serves as an Associate Editor for the *IEEE Transactions on Vehicular Technology*.

Francesco Pecile (SM'07) received the Doctor of Engineering Degree in electronics (cum laude) from the University of Udine in 2005. He is currently attending the Doctoral School in Industrial and Information Engineering at the Dipartimento di Ingegneria Elettrica, Gestionale e Meccanica (DIEGM) of the University of Udine. He is carrying out research activity in the telecommunication group, where he is gaining experience in the development of algorithms for wireless and powerline communications. He is co-author of seven conference papers.